

# Female Infertility Caused by Mutations in the Oocyte-Specific Translational Repressor *PATL2*

Sateesh Maddirevula,<sup>1,9</sup> Serdar Coskun,<sup>2,3,9</sup> Saad Alhassan,<sup>4</sup> Atif Elnour,<sup>5</sup> Hessa S. Alsaif,<sup>1</sup> Niema Ibrahim,<sup>1</sup> Firdous Abdulwahab,<sup>1</sup> Stefan T. Arold,<sup>6</sup> and Fowzan S. Alkuraya<sup>1,7,8,\*</sup>

Infertility is a relatively common disorder of the reproductive system and remains unexplained in many cases. *In vitro* fertilization techniques have uncovered previously unrecognized infertility phenotypes, including oocyte maturation arrest, the molecular etiology of which remains largely unknown. We report two families affected by female-limited infertility caused by oocyte maturation failure. Positional mapping and whole-exome sequencing revealed two homozygous, likely deleterious variants in *PATL2*, each of which fully segregates with the phenotype within the respective family. *PATL2* encodes a highly conserved oocyte-specific mRNP repressor of translation. Previous data have shown the strict requirement for *PATL2* in oocyte-maturation in model organisms. Data gathered from the families in this study suggest that the role of *PATL2* is conserved in humans and expand our knowledge of the factors that are necessary for female meiosis.

Infertility, a reproductive-system disorder defined by the failure to achieve a clinical pregnancy after 12 months or more of regular unprotected sexual intercourse, affects 10.7%–15.5% of couples.<sup>1</sup> Although infertility is highly heterogeneous in etiology, investigating the cause is necessary for guiding treatment options. Additionally, molecular understanding of infertility has the potential to reveal fundamental insight into human reproduction. This is particularly true when mechanical and hormonal causes are excluded and abnormal cellular phenotypes are observed, which is now possible with the advent of *in vitro* fertilization (IVF) techniques. One example is the discovery of *TLE6* and *PADI6* (MIM: 612399 and 610363, respectively) mutations causing failure of zygote cleavage, which revealed a critical role of the extracellular maternal complex and zygotic gene activation in humans and their conserved role in other species.<sup>2,3</sup>

The syndrome of oocyte maturation failure is an extremely rare cause of primary female infertility: only a few cases have been reported to date. This maturation arrest can represent failure to complete any of the various stages of meiosis I or II.<sup>4,5</sup> The resulting incompetence of the oocyte to be fertilized even with intracytoplasmic sperm injection poses a significant management challenge. Several mutants (typically mice) have been described as having a maturation-arrest phenotype.<sup>6–13</sup> These include *Cdc25b* and *Pde3a* knockouts (KOs) that arrest at the germinal vesicle (GV) stage, *Mei1*, *Cks2*, *Mlh1*, and *Lfng* KOs that arrest at meiosis I, and *Smc1b* and *Mos* KOs that arrest at meiosis II.<sup>6–13</sup> Interestingly, although some of these mutants are associated with female-limited

sterility, others (e.g., *Mei*, *Cks2*, *Mlh1*, and *Smc1b* mutants) display a sexually dimorphic infertility phenotype. No mutations, however, have been reported in the human orthologs of these genes in the context of infertility. Thus, it remains unknown what causes maturation arrest in human female individuals with infertility. In this study, we suggest that *PATL2* (MIM: 614661) mutations are one such etiology on the basis of human genetics data and the gene's established role in oocyte maturation in model organisms.

Affected individuals were recruited after providing informed consent under a research protocol approved by King Faisal Specialist Hospital and Research Center (KFSHRC) research advisory council 2121053. Meiosis I maturation arrest was defined as the failure of resumption of meiosis after controlled ovarian stimulation and follicular maturation triggering by luteinizing hormone and human chorionic gonadotropin. Venous blood samples were obtained from the index individuals and available relatives in each family for DNA extraction. For positional mapping, the Axiom SNP Chip (Affymetrix) platform was used for genome-wide genotyping. Runs of homozygosity (ROHs) > 1 Mb were considered surrogates of autozygosity by AutoSNPa.<sup>14</sup> Linkage analysis was performed with the easyLINKAGE package under a fully penetrant autosomal-recessive female-limited model.<sup>15</sup> For exome analysis, we selected the index individual from each family. The samples were prepared according to the preparation guide of the Agilent SureSelect Target Enrichment Kit, and the resulting libraries were sequenced with the Illumina HiSeq 2000 sequencer. The Genome Analysis Toolkit was used for variant calling. We considered only variants

<sup>1</sup>Department of Genetics, King Faisal Specialist Hospital and Research Center, Riyadh 11211, Saudi Arabia; <sup>2</sup>Department of Pathology and Laboratory Medicine, King Faisal Specialist Hospital and Research Center, Riyadh 11211, Saudi Arabia; <sup>3</sup>College of Medicine, Alfaisal University, Riyadh, Saudi Arabia; <sup>4</sup>Department of Obstetrics and Gynecology, King Faisal Specialist Hospital and Research Center, Riyadh 11211, Saudi Arabia; <sup>5</sup>Dr. Sulaiman Al Habib Medical Group, Olaya Complex, Riyadh 11643, Saudi Arabia; <sup>6</sup>King Abdullah University of Science and Technology, Computational Bioscience Research Center, Division of Biological and Environmental Sciences and Engineering, Thuwal 23955-6900, Saudi Arabia; <sup>7</sup>Department of Anatomy and Cell Biology, College of Medicine, Alfaisal University, Riyadh 11533, Saudi Arabia; <sup>8</sup>Saudi Human Genome Program, King Abdulaziz City for Science and Technology, Riyadh 11442, Saudi Arabia

<sup>9</sup>These authors contributed equally to this work

\*Correspondence: [falkuraya@kfshrc.edu.sa](mailto:falkuraya@kfshrc.edu.sa)  
<http://dx.doi.org/10.1016/j.ajhg.2017.08.009>

© 2017 American Society of Human Genetics.

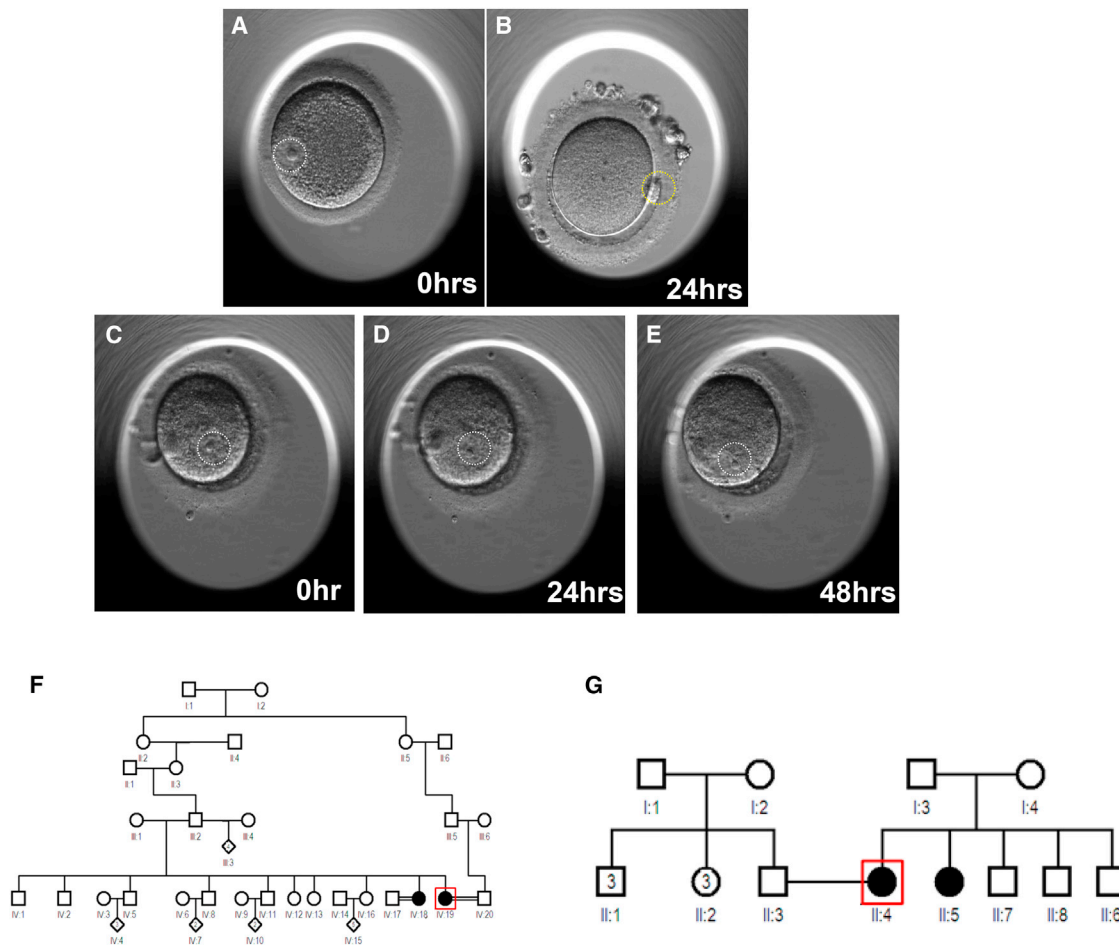


**Figure 1. Identification of Individuals with a Phenotype Involving Oocyte Maturation Arrest**

(A and B) Images of an immature oocyte with a germinal vesicle (A, white circle) and a mature oocyte with a polar body (B, yellow circle) from a normal woman.

(C–E) Images of immature oocytes from the individual with a maturation arrest phenotype from family 1. (C) An oocyte retrieved from a stimulated ovary. (D and E) Immature oocytes after 24 (D) and 48 (E) hr culture in *in vitro* maturation media indicate failure in maturation. Pedigrees of family 1 (F) and family 2 (G) are shown. WES was performed on the index individual (indicated by a red box) in each family.

that are novel or very rare (minor allele frequency [MAF] < 0.001) in the ExAC Browser and 2,379 Saudi exomes. We also performed computational structural analysis of candidate variants. Sequences were retrieved from UniProt. We used SwissModel to produce homology models.<sup>16</sup> RaptorX was used for prediction of secondary structures and protein disorders.<sup>17</sup> Models were manually inspected, and mutations were evaluated with PyMOL.

Family 1 consists of two Arab sisters (IV:18 and IV:19, currently 35 and 27 years of age, respectively) who presented with primary infertility but regular menstrual cycles to our IVF center at KFSHRC. The index individual (IV:19) had a 7-year history of primary infertility. She had undergone seven failed IVF cycles, each with an adequate number of retrieved eggs (5–23 oocytes), but all arrested in meiosis I, as indicated by the presence of a GV (Figures 1C–1E, Movie S1, and Supplemental Note; Figures 1A and 1B and Movie S2 show normal meiosis I for comparison). Hormone levels were measured on the third day of the

cycle, and her follicle-stimulating hormone (FSH) level was 6.6 IU/L. There was no indication of polycystic ovary disorder on hormonal or imaging studies. Oocytes were cultured in the *in vitro* maturation media, but there was no progress on meiotic maturation for 48 hr. Her sister (IV:18) also had a 6-year history of primary infertility. She had undergone one IVF cycle, and four retrieved eggs were arrested in meiosis I (Figures S1A–S1C). Like her sister, she lacked features of polycystic ovary disorder, and her FSH level was 5.6 IU/L on the third day of the cycle. Although consanguinity was denied, both parents belong to the same tribe. Please refer to the Supplemental Note for detailed clinical information.

Family 2 also consists of two Arab sisters with primary infertility. The index individual (II:4), 33 years old, presented to the IVF center at Habib Medical Group Hospital and underwent five trials of failed intrauterine insemination followed by an unsuccessful IVF cycle. A total of 20 oocytes were retrieved, but none were mature

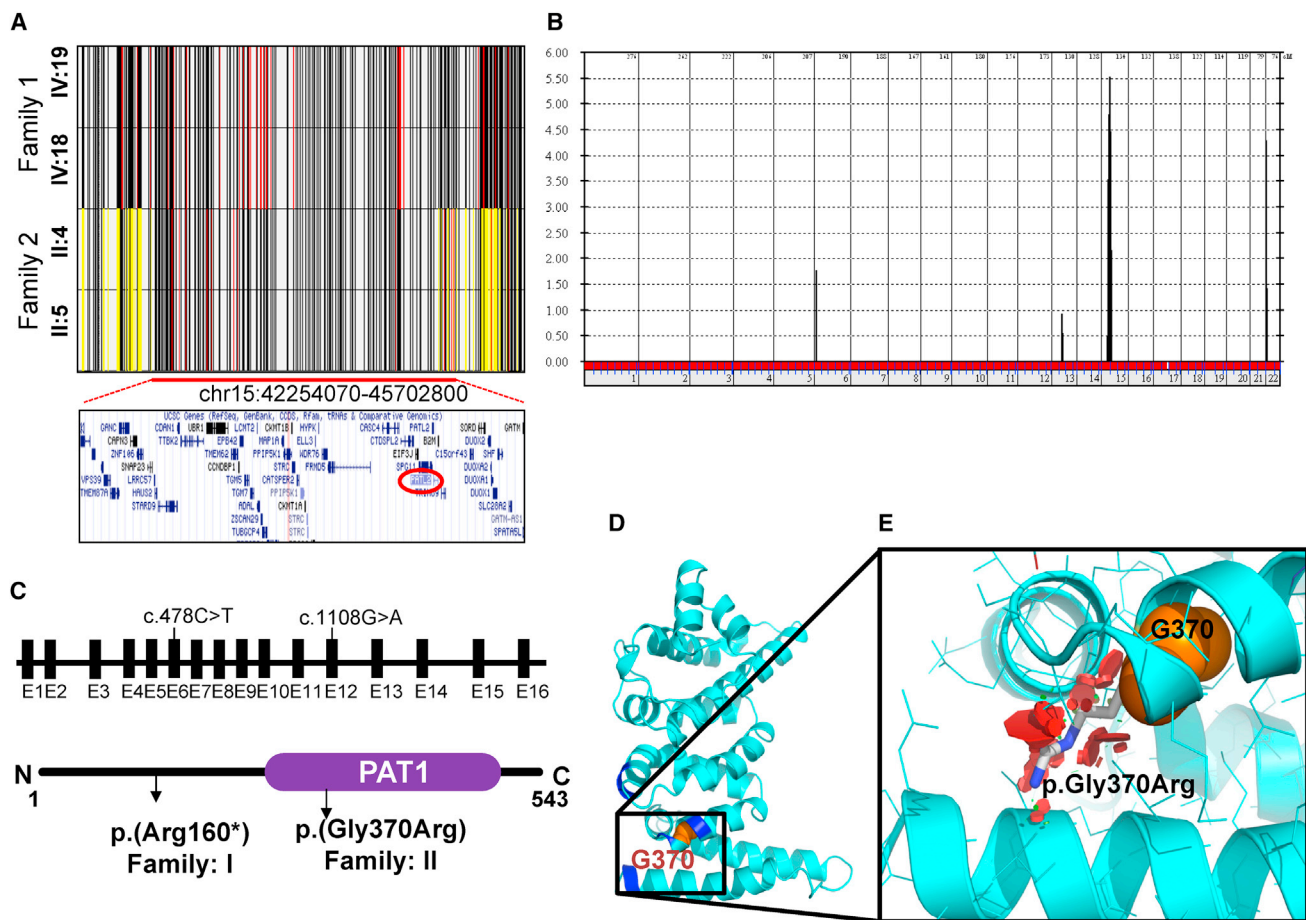


**Figure 2. Identification of *PATL2* Variants in Individuals with a Phenotype Involving Oocyte Maturation Arrest**

(A) Shared haplotypes (chr15: 42,254,070–45,702,800; UCSC Genome Browser hg19) of the affected members from family 1 (IV:19 and IV:18) and family 2 (II:4 and II:5). Yellow lines indicate heterozygous SNPs. Red lines indicate rare homozygous SNPs. The lower panel shows genes that are within the shared ROH region. The position of *PATL2* (chr15: 44,966,961–45,003,514; UCSC Genome Browser hg19) is highlighted with a red circle.

(B) Genome-wide linkage analysis showing a chr15 peak with a pLOD score of 5.5 (16 individuals are included; see Figure S2 for details).

(C) Genomic context and structural presentation of *PATL2*, including the two variants.

(D and E) The PAT1 domain contains the residues (Arg301, Leu302, Arg368, Ala327, Arg402, and Arg403) corresponding to the PATL1 residues involved in RNA binding (shown in dark blue). (D) Based on the structure of the corresponding region of PATL1 (PDB: 2XEQ; 34% sequence identity), the secondary-structure representation of the homology model of the C-terminal domain of PATL2 (residues 299–540) is shown. Gly370 is shown as orange spheres. (E) Magnified view of the outlined region in (D). In addition to Gly370 (orange), the putative p.Gly370Arg rotamer side chain (gray) with the least possible clashes (red discs) is shown, illustrating that p.Gly370Arg compromises the folding and function of PATL2.

(Figure S1D). She was noted to have a failure of resumption of meiotic arrest. Her sister, 26 years old, has a 3-year history of primary infertility but has not yet had any IVF cycles. Both sisters had regular menstrual cycles, and their workups ruled out polycystic ovary disorder. Similar to the parents in family 1, the sisters' parents are not consanguineous but have the same tribal origin.

Given the extreme rarity of their phenotype, we hypothesized that both families are affected by a similar underlying molecular defect. Although neither family is apparently consanguineous, the shared tribal origin of the parents (endogamy) makes it still possible that the phenotype is caused by autozygosity for ancestral recessive mutations, which can be traced by positional mapping. Examina-

tion of the ROHs revealed only one overlapping autozygous region of 3.4 Mb (chr15: 42,254,070–45,702,800) (Figure 2A). Linkage analysis confirmed that both families map to this candidate locus (Figure 2B). However, the haplotype of the affected members was clearly different between the two families, which suggests that each family has a different mutation in the candidate gene, consistent with the difference in their tribal affiliation (Figure 2A and Table S1). Exome sequencing revealed 63,890 variants in the index individual of family 1 and 72,370 variants in the index individual of family 2. However, only one rare homozygous variant was identified within the candidate locus in each family, and both variants involved *PATL2*: c.478C>T (p.Arg160\*) (GenBank: NM\_001145112.1) in family 1 and c.1108G>A (p.Gly370Arg) (GenBank: NM\_001145112.1)

in family 2 (Table S2). No other candidate homozygous variants outside the linkage interval or compound-heterozygous variants were identified. Segregation analysis using Sanger sequencing confirmed that the variant is homozygous in the affected members of each respective family (Figure S2). Interestingly, homozygosity for c.478C>T (p.Arg160\*) was compatible with fertility in males, as demonstrated by the father and two brothers in family 1 (Figure S2A). Both variants were completely absent in 2,379 Saudi exomes and very rare or absent in the ExAC Browser (MAF = 0.00003362 and 0 for p.Arg160\* and p.Gly370Arg, respectively).

*PATL2* encodes an RNA-binding protein that acts as a translational repressor. PAT proteins contain a conserved N-terminal sequence, a proline-rich region, a Mid domain, and a C-terminal domain. Prediction of secondary structure and disorder indicated that the N-terminal 290 residues of the 541-residue protein *PATL2* are highly mobile and unstructured. The *PATL2* residues 299–540 are predicted to adopt a stable three-dimensional (3D) fold. A 3D structure of this C-terminal domain can be modeled with good confidence on the basis of the 34% identical C-terminal domain of *PAT1* (PDB: 2XES and 2XEQ; modeling QMEAN score of  $-2.79$ ). Gly370 localizes in helix 3 of the C-terminal domain. It is oriented toward the hydrophobic core of the superhelical fold of this domain (Figure 2D). An arginine in this position would result in severe steric clashes (Figure 2E) and lead to the unfavorable introduction of a charge within the hydrophobic core. The p.Gly370Arg variant is therefore expected to strongly destabilize this protein region (PolyPhen-2: 0.915; SIFT: 0.03; and CADD: 33). In *PAT1*, this region is involved in RNA binding.<sup>18</sup> This region is highly conserved, and stereochemical features are preserved in *PATL2* (Figures 2D and 2E). It is therefore expected that p.Gly370Arg will lead to loss of RNA and protein ligands that are central to the function of PAT proteins. The glycine residue at the 370<sup>th</sup> position is highly conserved from humans to yeast (Figure S3). The premature stop codon at position 160, on the other hand, leads to complete loss of the RNA-binding domain, so this truncation is expected to result in severe loss of function of *PATL2* (we found no evidence of nonsense-mediated decay).

In humans, oogenesis commences *in utero* and stalls in meiosis I until ovulation (when meiosis I is completed), whereas meiosis II is completed only after fertilization. During this process, the chromatin condensation does not permit active transcription; as a result, intracellular signaling is primarily controlled at the translational level. A pivotal factor in this process is a large mRNP complex that sequesters RNA in the oocyte.<sup>19</sup> This complex is functionally very similar to the P bodies in the somatic cells.<sup>20,21</sup> Completion of meiosis is marked by GV breakdown (GVBD), a critical event that is triggered by a marked decline in CPEB and consequent translational activation of *MOS* (MIM: 190060) and *CCNB1* (MIM: 123836).<sup>22–24</sup>

Interestingly, *Mos* deficiency has been shown to result in meiosis arrest in mice.<sup>25</sup>

*PATL2* and *PATL1* are vertebrate paralogs of *Pat1p* in yeast, *PATR-1* in roundworm, and *Hpat* in fruit fly.<sup>26</sup> The ancestral ortholog served a dual function (RNA decapping and translational repression), and its deficiency has been shown to result in translational repression with deleterious consequences.<sup>27</sup> *PATL2* was first identified in 1992 as a *Xenopus* oocyte-specific protein that binds single-stranded DNA, and it was labeled P100.<sup>28</sup> It was later found that *PATL2* is a component of a complex involving the cytoplasmic polyadenylation element and its binding factor CPEB, and this complex is a critical temporal regulator of translation during oocyte maturation.<sup>26,29</sup> *PATL2* is highly abundant in early stages of meiosis but declines precipitously, similarly to CPEB (with which it physically interacts), with the onset of GVBD. Indeed, it has been shown that this decline in the amount of *PATL2* is necessary for GVBD and that ectopic expression completely blocks meiosis I progression.<sup>26,30</sup> Importantly, *PATL1* does not compensate for the role of *PATL2* in meiosis given that it is only detectable in later stages. *PATL2* has been shown to harbor RNA binding activity and resulting translational repression, but decapping activity has not been shown.<sup>26</sup> On *PATL1*, the region necessary for RNA binding has been shown to involve a basic patch on the C-terminal domain (residues Arg519, Arg520, Arg591, Arg595, Lys625, and Lys626, corresponding to Arg301, Leu302, Arg368, Ala327, Arg402, and Arg403, respectively, in *PATL2*);<sup>18</sup> this patch is completely lost as a result of the truncating variant in family 1 and is expected to be severely impaired by the missense variant in family 2.

The function of *PATL2* in humans is unknown. Despite the inbred nature of the local population, the complete lack of homozygous deleterious variants in our local exome database suggests that it is highly constrained in the recessive sense. Indeed, the data we present in this study suggest a role in human oogenesis that is only lost in the setting of biallelic mutations. Although data from *Xenopus* indicate that the decline in the amount of *PATL2* ortholog coincides with and probably triggers GVBD, we show that its deficiency in humans results in a highly similar meiosis I arrest. This suggests a strict requirement for temporal control of the *PATL2* expression level for normal oocyte maturation. Interestingly, we show that the effect of *PATL2* is limited to females, given that at least three males who are homozygous for a severe truncating variant are fertile.

In conclusion, we suggest that *PATL1* mutations arrest meiosis I and thus lead to female-limited infertility in humans. This rare etiology of infertility expands our knowledge of factors required for normal human oogenesis and suggests a highly conserved network that controls this process across species. We hope that this and future discoveries of the molecular underpinning of human infertility will inform and advance new therapeutic strategies.

## Supplemental Data

Supplemental Data include a Supplemental Note, three figures, two tables, and two movies and can be found with this article online at <http://dx.doi.org/10.1016/j.ajhg.2017.08.009>.

## Acknowledgments

We thank the study participants for their enthusiastic participation. We also thank the Sequencing and Genotyping Core Facilities at the King Faisal Specialist Hospital and Research Center for their technical help. This work was funded in part by the King Abdulaziz City for Science and Technology (13-BIO1113-20), and we acknowledge the support of the Saudi Human Genome Project. The research reported by S.T.A. in this publication was supported by funding from the King Abdullah University of Science and Technology.

Received: June 14, 2017

Accepted: August 11, 2017

Published: September 28, 2017

## Web Resources

CADD, <http://cadd.gs.washington.edu/home>

ClustalW2, <http://www.ebi.ac.uk/Tools/msa/clustalw2/>

Exome Aggregation Consortium (ExAC) Browser, <http://exac.broadinstitute.org/>

GenBank, <https://www.ncbi.nlm.nih.gov/genbank/>

OMIM, <http://www.omim.org>

PolyPhen-2, <http://genetics.bwh.harvard.edu/pph2/>

PyMOL, <http://pymol.org/>

RaptorX, <http://raptorx.uchicago.edu/>

RCSB Protein Data Bank, <http://www.rcsb.org/pdb/home/home.do>

UCSC Genome Browser, <http://genome.ucsc.edu>

UniProt, <http://www.uniprot.org/>

## References

1. Thoma, M.E., McLain, A.C., Louis, J.F., King, R.B., Trumble, A.C., Sundaram, R., and Buck Louis, G.M. (2013). Prevalence of infertility in the United States as estimated by the current duration approach and a traditional constructed approach. *Fertil. Steril.* *99*, 1324–1331.e1.
2. Alazami, A.M., Awad, S.M., Coskun, S., Al-Hassan, S., Hijazi, H., Abdulwahab, F.M., Poizat, C., and Alkuraya, F.S. (2015). TLE6 mutation causes the earliest known human embryonic lethality. *Genome Biol.* *16*, 240.
3. Maddirevula, S., Coskun, S., Awartani, K., Alsaif, H., Abdulwahab, F.M., and Alkuraya, F.S. (2017). The human knockout phenotype of PADI6 is female sterility caused by cleavage failure of their fertilized eggs. *Clin. Genet.* *91*, 344–345.
4. Beall, S., Brenner, C., and Segars, J. (2010). Oocyte maturation failure: a syndrome of bad eggs. *Fertil. Steril.* *94*, 2507–2513.
5. Mrazek, M., and Fulka Jr, J., Jr. (2003). Failure of oocyte maturation: possible mechanisms for oocyte maturation arrest. *Hum. Reprod.* *18*, 2249–2252.
6. Lincoln, A.J., Wickramasinghe, D., Stein, P., Schultz, R.M., Palko, M.E., De Miguel, M.P., Tessarollo, L., and Donovan, P.J. (2002). Cdc25b phosphatase is required for resumption of meiosis during oocyte maturation. *Nat. Genet.* *30*, 446–449.
7. Masciarelli, S., Horner, K., Liu, C., Park, S.H., Hinckley, M., Hockman, S., Nedachi, T., Jin, C., Conti, M., and Manganiello, V. (2004). Cyclic nucleotide phosphodiesterase 3A-deficient mice as a model of female infertility. *J. Clin. Invest.* *114*, 196–205.
8. Libby, B.J., De La Fuente, R., O'Brien, M.J., Wigglesworth, K., Cobb, J., Inselman, A., Eaker, S., Handel, M.A., Eppig, J.J., and Schimenti, J.C. (2002). The mouse meiotic mutation *mei1* disrupts chromosome synapsis with sexually dimorphic consequences for meiotic progression. *Dev. Biol.* *242*, 174–187.
9. Spruck, C.H., de Miguel, M.P., Smith, A.P., Ryan, A., Stein, P., Schultz, R.M., Lincoln, A.J., Donovan, P.J., and Reed, S.I. (2003). Requirement of Cks2 for the first metaphase/anaphase transition of mammalian meiosis. *Science* *300*, 647–650.
10. Edelmann, W., Cohen, P.E., Kane, M., Lau, K., Morrow, B., Bennett, S., Umar, A., Kunkel, T., Cattoretti, G., Chaganti, R., et al. (1996). Meiotic pachytene arrest in MLH1-deficient mice. *Cell* *85*, 1125–1134.
11. Hahn, K.L., Johnson, J., Beres, B.J., Howard, S., and Wilson-Rawls, J. (2005). Lunatic fringe null female mice are infertile due to defects in meiotic maturation. *Development* *132*, 817–828.
12. Revenkova, E., Eijpe, M., Heyting, C., Hodges, C.A., Hunt, P.A., Liebe, B., Scherthan, H., and Jessberger, R. (2004). Cohesin SMC1  $\beta$  is required for meiotic chromosome dynamics, sister chromatid cohesion and DNA recombination. *Nat. Cell Biol.* *6*, 555–562.
13. Araki, K., Naito, K., Haraguchi, S., Suzuki, R., Yokoyama, M., Inoue, M., Aizawa, S., Toyoda, Y., and Sato, E. (1996). Meiotic abnormalities of *c-mos* knockout mouse oocytes: activation after first meiosis or entrance into third meiotic metaphase. *Biol. Reprod.* *55*, 1315–1324.
14. Carr, I.M., Flintoff, K.J., Taylor, G.R., Markham, A.F., and Bonthron, D.T. (2006). Interactive visual analysis of SNP data for rapid autozygosity mapping in consanguineous families. *Hum. Mutat.* *27*, 1041–1046.
15. Lindner, T.H., and Hoffmann, K. (2005). easyLINKAGE: a PERL script for easy and automated two-/multi-point linkage analyses. *Bioinformatics* *21*, 405–407.
16. Arnold, K., Bordoli, L., Kopp, J., and Schwede, T. (2006). The SWISS-MODEL workspace: a web-based environment for protein structure homology modelling. *Bioinformatics* *22*, 195–201.
17. Källberg, M., Margaryan, G., Wang, S., Ma, J., and Xu, J. (2014). RaptorX server: a resource for template-based protein structure modeling. *Methods Mol Biol.* *1137*, 17–27.
18. Braun, J.E., Tritschler, F., Haas, G., Igreja, C., Truffault, V., Weichenrieder, O., and Izaurrealde, E. (2010). The C-terminal  $\alpha$ - $\alpha$  superhelix of Pat is required for mRNA decapping in metazoa. *EMBO J.* *29*, 2368–2380.
19. Bouvet, P., and Wolffe, A.P. (1994). A role for transcription and FRGY2 in masking maternal mRNA within *Xenopus* oocytes. *Cell* *77*, 931–941.
20. Parker, R., and Sheth, U. (2007). P bodies and the control of mRNA translation and degradation. *Mol. Cell* *25*, 635–646.
21. Kotaja, N., and Sassone-Corsi, P. (2007). The chromatoid body: a germ-cell-specific RNA-processing centre. *Nat. Rev. Mol. Cell Biol.* *8*, 85–90.
22. Ballantyne, S., Daniel, D.L., Jr., and Wickens, M. (1997). A dependent pathway of cytoplasmic polyadenylation reactions

- linked to cell cycle control by c-mos and CDK1 activation. *Mol. Biol. Cell* 8, 1633–1648.
23. de Moor, C.H., and Richter, J.D. (1997). The Mos pathway regulates cytoplasmic polyadenylation in *Xenopus* oocytes. *Mol. Cell. Biol.* 17, 6419–6426.
  24. Radford, H.E., Meijer, H.A., and de Moor, C.H. (2008). Translational control by cytoplasmic polyadenylation in *Xenopus* oocytes. *Biochimica et Biophysica Acta*, 217–2229.
  25. Colledge, W.H., Carlton, M.B., Udy, G.B., and Evans, M.J. (1994). Disruption of c-mos causes parthenogenetic development of unfertilized mouse eggs. *Nature* 370, 65–68.
  26. Marnef, A., Maldonado, M., Bugaut, A., Balasubramanian, S., Kress, M., Weil, D., and Standart, N. (2010). Distinct functions of maternal and somatic Pat1 protein paralogs. *RNA* 16, 2094–2107.
  27. Haas, G., Braun, J.E., Igreja, C., Tritschler, F., Nishihara, T., and Izaurralde, E. (2010). HPat provides a link between deadenylation and decapping in metazoa. *J. Cell Biol.* 189, 289–302.
  28. Rother, R.P., Frank, M.B., and Thomas, P.S. (1992). Purification, primary structure, bacterial expression and subcellular distribution of an oocyte-specific protein in *Xenopus*. *Eur. J. Biochem.* 206, 673–683.
  29. Hake, L.E., and Richter, J.D. (1994). CPEB is a specificity factor that mediates cytoplasmic polyadenylation during *Xenopus* oocyte maturation. *Cell* 79, 617–627.
  30. Nakamura, Y., Tanaka, K.J., Miyauchi, M., Huang, L., Tsujimoto, M., and Matsumoto, K. (2010). Translational repression by the oocyte-specific protein P100 in *Xenopus*. *Dev. Biol.* 344, 272–283.

**The American Journal of Human Genetics, Volume 101**

**Supplemental Data**

**Female Infertility Caused by Mutations**

**in the Oocyte-Specific Translational Repressor *PATL2***

**Sateesh Maddirevula, Serdar Coskun, Saad Alhassan, Atif Elnour, Hessa S. Alsaif, Niema Ibrahim, Firdous Abdulwahab, Stefan T. Arold, and Fowzan S. Alkuraya**

## Supplemental Note

### Case #1 (Family 1\_IV:19):

23 years old lady with primary infertility for 7 years. Married to a 29 years old gentleman.

#### Gynecological history:

Normal menarche, regular cycles, no hirsutism, no acne or galactorrhea no dysmenorrhea, no history of PID, endometriosis, or pelvic surgeries. Not on any hormonal treatment or contraception.

#### Family history:

She gave history of similar infertility concerns in one of her younger sisters (see Case #2 below).

#### Previous fertility assessment diagnosis & treatment:

- Hormonal profile: hyperprolactinemia on bromocriptine 1.25mg PO OD, last prolactin level 49. FSH = 5.3. LH = 12.4. TSH 5.99
- Underwent 6 ovulation induction cycles via clomiphene citrate. Then 5 ovulation inductions by gonadotropins with timed intercourse.

#### Partner history:

29 years old gentleman who is medically & surgically free. Not using any medication. Doesn't have any allergies. Non-smoker.

Semen analysis: 6.3 ml, 25 mil/ml, 38% motile, 96% abnormal forms, TMC = 58.950000, acrosome deficiencies 59%

#### Workup:

- Weight = 44 Kg, Height = 146 cm, BMI = 20.6
- Blood group A+
- Hb = 116 g/L
- FSH = 6.6 IU/L
- LH = 5.5 IU/L
- Estradiol level = 150 pmol/L
- TSH = 2.8
- Prolactin level = 14.5



- Rubella Immune
- AFC 10 +6
- HSG films reviewed: Right tubal block with normal left tube & cavity

**Infertility diagnosis: Unexplained Infertility**

**Infertility treatment offered & outcome:**

**A. Super ovulation: had 2 cycle of super ovulation IUI as follows:**

**Cycle #1:** → Super ovulation – IUI HMG 150 IU for 6 days then increased to 187.5 IU for 5 days + 200mcg Buserlin. Had 2 follicles recruited 1 was 18 mm & the other was 15 mm. Endometrium started 2 mm became 12 mm at trigger day. Triggered oocyte maturation by 10,000 IU HCG. IUI was performed smoothly with no complications or difficulties. For luteal phase support progesterone pessary prescribed 200 mg vaginally BID for 14 days. Pregnancy test negative.

**Cycle #2:** → Super ovulation – IUI HMG 187.5 IU for 11 days + 200mcg Buserlin. Had 2 follicles recruited 1 was 18 mm & the other was 16 mm. endometrium started 2 mm became 13 mm at trigger day. Triggered oocyte maturation by 10,000 IU HCG. IUI was performed smoothly with no complications or difficulties. For luteal phase support progesterone pessary prescribed 200 mg vaginally BID for 14 days. Pregnancy test negative.

**B. IVF Treatment: had total of 7 cycles as follows:**

**Summary of cycles:**

**Cycle #1:** → Long protocol with leuprolide 3.75 IM once at follicular phase at cycle day → HMG Menogon 225 IU for 13 days then 75 IU for 1 days → triggered 10,000 IU HCG (Endometrial thickness 16mm) → 11 oocytes collected → all were GV

**Cycle #2:** → Short protocol → started at cycled day 4 → HMG Menogon 150 IU for 9 days then 225 IU for 5 days + Buserlin 400 mcg SC daily → triggered 10,000 IU HCG (Endometrial thickness 13mm) → 4 oocytes collected (only right ovary, left ovary not aspirated due to bladder accessibility) → all were GV

**Cycle #3:** → Long protocol (we wanted to try GnRH flexible Antagonist protocol but we didn't have antagonist in the hospital & patient couldn't afford it from outside) had leuprolide 3.75 IM once at follicular phase at cycle day → HMG Menogon 225 IU for 9 days then 300 IU for 5 days → triggered 10,000 IU HCG (Endometrial thickness 16mm) → 21 oocytes collected → all were GV

**Cycle #4:** → Short protocol → started at cycled day 4 → HMG Menogon 300 IU for 12 days → after 10 days of stimulation a leading follicle reached 15m, (LH measured on same day 5.9 iu/L, next day 3.3 iu/L the day after 3 iu/L ) → triggered Buserelin 500 mcg SC (Endometrial thickness 14mm) → 5 oocytes collected → all were GV

**Cycle #5:** → Short protocol → started at cycled day 3 → HMG Menogon 300 IU for 6 days then 375 IU for 4 days then increased to 450 IU 2 days + Buserlin 400 mcg SC daily → triggered 10,000 IU HCG (Endometrial thickness 14mm) → 2 oocytes collected → all were GV

**Cycle #6:** → Flexible antagonist protocol → started at cycled day 4 → FSH Gonal-F 300 IU for 9 days then antagonist started 0.5 Orgalotran both continued 3 days (developed 2 right hemorrhagic cyst at CD 10 ) → triggered by Superfact 0.4 ml SC (Endometrial thickness 18mm) → 13 oocytes collected → all were GV

**Cycle #7:** → Flexible antagonist protocol → started at cycled day 3 → FSH Gonal-F 300 IU for 10 days then antagonist started 0.5 Orgalotran both continued 3 days → triggered by Superfact 0.4 ml SC & HCG 10,000 IU SC (Endometrial thickness 18mm) → had 22 follicles recruited 23 oocytes collected → 14 eggs were GV's & 7 eggs degenerated.

## **Case #2 (Family 2\_IV:18):**

25 years old lady with primary infertility for 6 years, married to a 31 years old gentleman.

### **Gynecological history:**

Menarche at age of 12, cycles range 28 – 35 days with flow 5-6 days, no acne or galactorrhea, mild dysmenorrhea & no history of PID, endometriosis, pelvic surgeries. Not on any hormonal treatment or contraception.

**Past medical history:** free

**Past surgical history:** free

**Medications:** None

**Allergies:** None

### **Partner history:**

He's known to be diabetic controlled on oral hypoglycemic agents. Surgically free. Doesn't have any allergies. Nonsmoker.

### **Workup:**

- Weight = 59.7 Kg, Height = 158 cm, BMI = 23.9
- Blood group A+
- Hb = 123 g/L
- FSH = 5.6 IU/L
- LH = 14.7 IU/L
- Estradiol level = 189 pmol/L
- TSH = 2.29
- Prolactin level = 14.79
- Rubella Immune
- AFC 15+20
- Semen analysis: 1 ml, 162 mil/ml, 72% motile, 1% normal forms, TMC = 116.640000, acrosome deficiencies 77%
- HSG films reviewed: normal cavity & patent tubes

**Infertility diagnosis:** Unexplained Infertility

**Infertility treatment offered & outcome:**

1. **Short protocol** → started at cycled day 3 → HMG Menogon 150 IU for 6 days then 75 IU for 5 days then increased to 150 IU for 2 days + Buserlin 400 mcg SC daily → triggered 10,000 IU HCG (Endometrial thickness 8mm) → 4 oocytes collected → all were GV

**Figure S1**

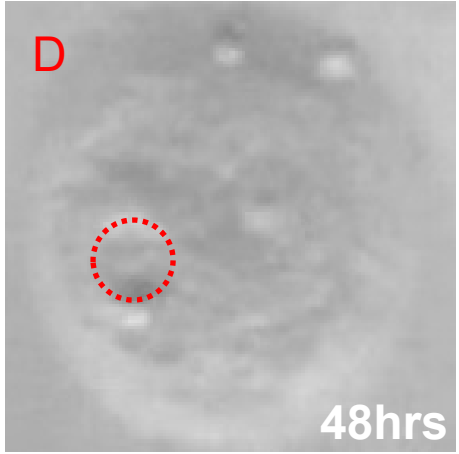
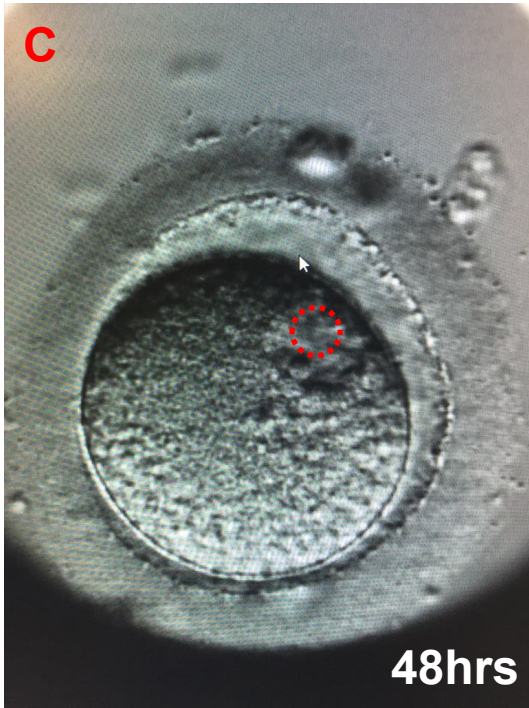
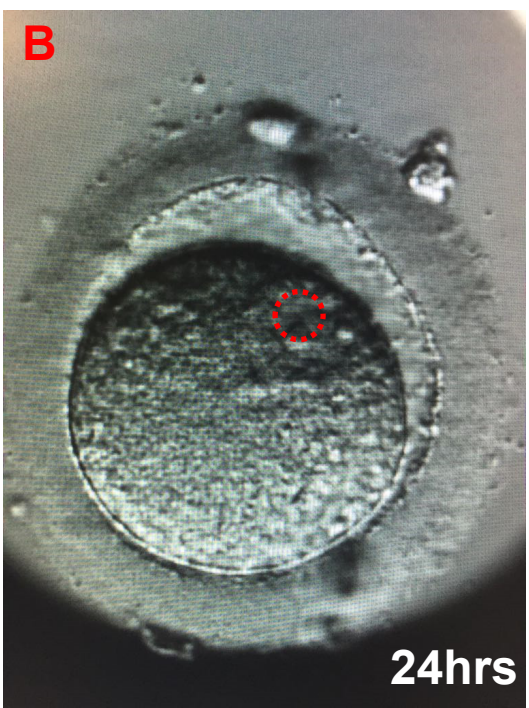
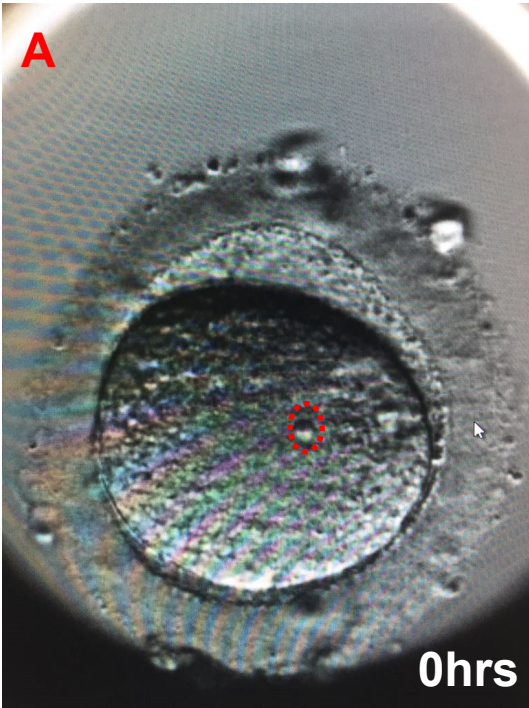


**Figure S1.** A-C) Images of immature oocytes from the individual IV:18 in family 1 with maturation arrest phenotype from family 1. Red circles indicate germinal vesicles.

D) Images of immature oocytes from individual II:4 in family 2 showing a similar defect despite the much lower quality of the image.

Figure S2

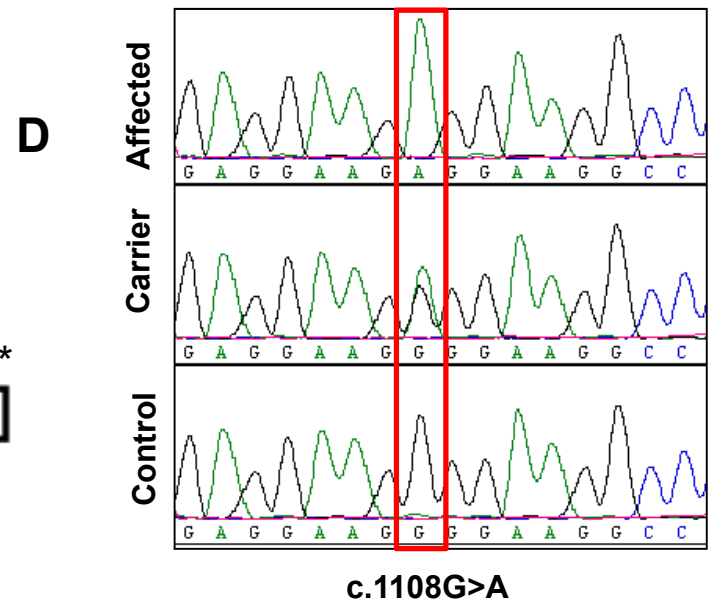
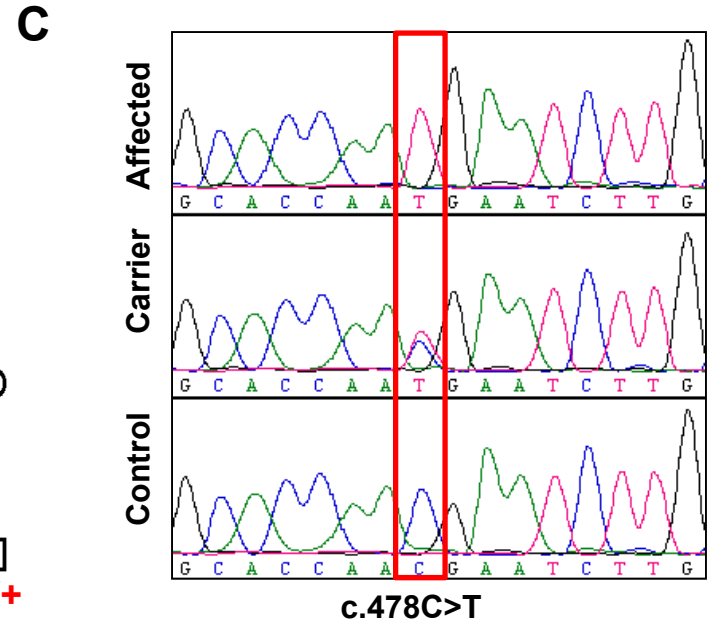
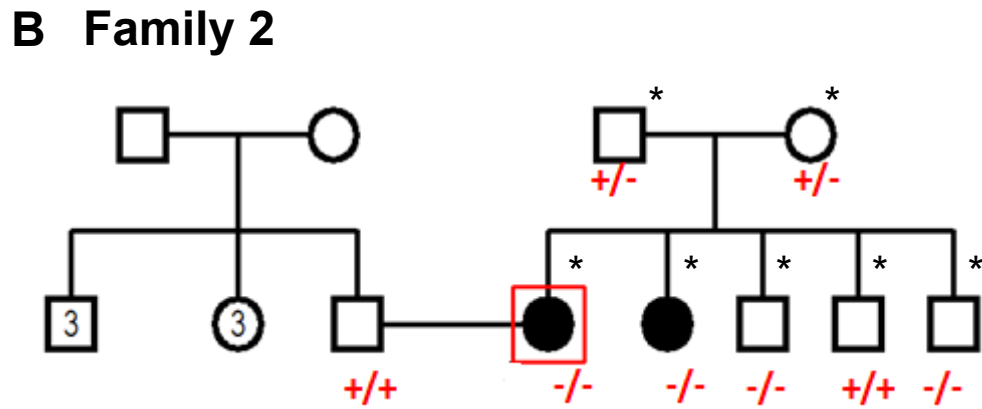
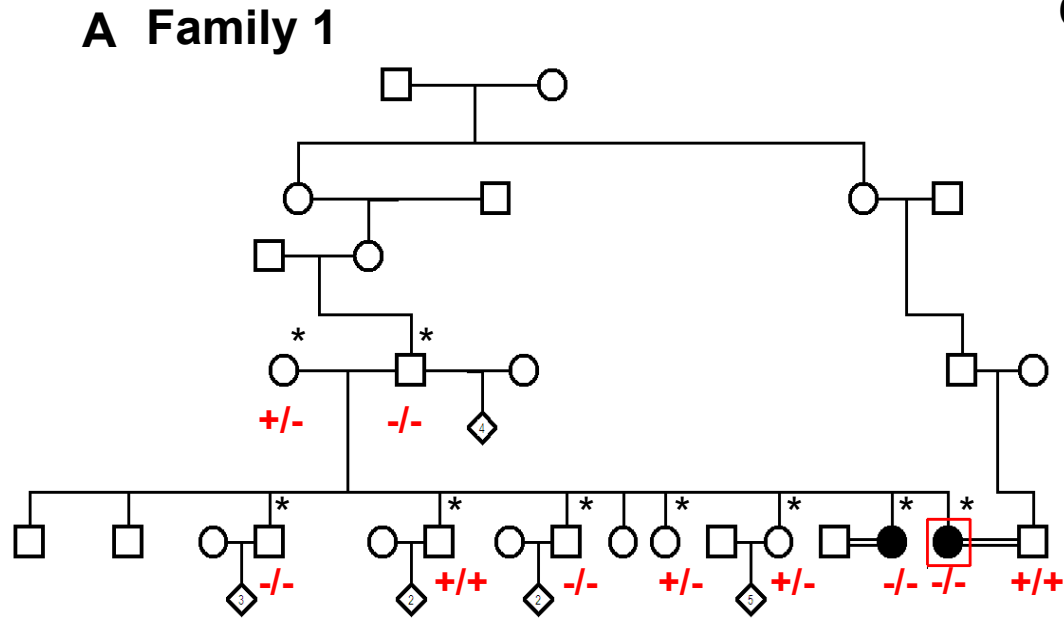


**Figure S2.** Pedigrees of family1 (A) and family 2 (B) showing the *PATL2* mutation status. Red box indicates index for whom whole exome sequence (WES) was performed. Segregation was performed for the available family members. -/- denotes homozygous status; +/- denotes carrier status; +/+ denotes wild type; \* marks individuals included in the linkage analysis. C) Chromatogram for the mutation c.478C>T:p.(Arg160\*) in family 1. D) Chromatogram for the mutation c.1108G>A:p.(Gly370Arg) in family 2.



Figure S3

Yeast	LHI---DDSSYDVNPFISMLSFDKGIKIMPRIFNFLDKQQ
C.elegans	-----VIINELMGDDLKLMQMSKGRAVITRTLKVVEPRD
Drosophila	--LVNKLKAGLAFDKVIAMMNVRKGIKILIRRIMPFIADQS
Zebrafish	L---RCTNLD-SGEEFLSCLLVSKGKRLVARLLPFLSHDS
Xenopus	LNMAPCHSEDESENEFLQLLQVGKGGKLIARLLPFLTRVQ
Mouse	LKTQEQNNLEEAADNLLQVLSVRKGGKVLVARLLPFLPPDQ
Cattle	LKAQGQNNLEAADDGFLQALSVGKGGKALVARLLPILPRDR
Dog	LKTQEQKNLEEAADGFLQVLSVRKGGKALVARLLPFLPQDQ
Chimpanzee	LKTQEQNNLEEAADGFLQVLSVRKGGKALVARLLPFLPQDQ
Human	LKTQEQNNLEEAADGFLQVLSVRKGGKALVARLLPFLPQDQ

**Gly370Arg**

**Figure S3.** The glycine 370 residue of PATL2 is highly conserved from human to yeast. Protein sequences were obtained publically available genomic databases: human (NM\_001145112.1), chimpanzee (XM\_001146504.2), dog (XM\_003640026.1), cattle (XM\_002691093.2), mouse (NM\_026251.2), *Xenopus* (NP\_001135679.1), zebrafish (XP\_683261.4), *Drosophila* (NP\_001287369.1), *C.elegans* (NP\_496514.1) and yeast (NP\_010002.3). PATL2 protein sequences were aligned by using ClustalW.

**Table S1: list of haplotypes from two families with in the shared ROH (chr15:42,254,070-45,702,800).**

SNP	Mb distance	Family 1 IV:19	Family 1 IV:18	Family 2 II:4	Family 2 II:5
RS2925339	42091212	ab	ab	BB	BB
RS1618332	42184794	ab	ab	BB	BB
RS1048166	42192040	ab	ab	AA	AA
RS8041458	42196846	ab	ab	BB	BB
RS17686769	42205483	ab	ab	BB	BB
RS4923919	42208041	ab	ab	AA	AA
RS2899033	42212047	BB	BB	BB	BB
RS10518742	42220257	BB	BB	BB	BB
RS1648856	42233912	AA	AA	BB	BB
RS1648855	42237403	AA	AA	BB	BB
RS34899815	42254068	BB	BB	AA	AA
RS1868831	42257929	AA	AA	AA	AA
RS1704345	42270697	ab	ab	AA	AA
RS4924593	42273259	ab	ab	AA	AA
RS1668572	42273526	ab	ab	BB	BB
RS1704352	42281805	BB	BB	BB	BB
RS7175837	42300303	ab	ab	BB	BB
RS1704367	42300475	BB	BB	BB	BB
RS12438854	42300886	ab	ab	AA	AA
RS9919954	42302520	ab	ab	AA	AA
RS7182446	42302751	BB	BB	BB	BB
RS12439430	42305042	ab	ab	BB	BB
RS12909362	42315401	AA	AA	BB	BB
RS2665203	42316527	BB	BB	BB	BB
RS2724943	42319233	ab	ab	AA	AA
RS4924608	42332784	ab	ab	AA	AA
RS1668596	42336250	BB	BB	AA	AA
RS7175879	42336450	BB	BB	BB	BB
RS1712436	42338079	BB	BB	BB	BB
RS1993069	42339158	ab	ab	BB	BB
RS12902878	42343794	ab	ab	BB	BB
RS776688	42345046	ab	ab	AA	AA
RS16972565	42350013	BB	BB	BB	BB
RS776699	42350037	BB	BB	BB	BB
RS1668588	42364362	BB	BB	BB	BB
RS59107494	42366224	AA	AA	BB	BB
RS7166111	42368506	ab	ab	BB	BB
RS2412657	42387203	BB	BB	AA	AA
RS8028204	42392164	AA	AA	BB	BB
RS17748385	42395956	AA	AA	AA	AA
RS12050606	42396187	ab	ab	BB	BB
RS1008979	42399642	AA	AA	BB	BB
RS2122677	42400066	AA	AA	AA	AA
RS675996	42400764	ab	ab	AA	AA
RS28665345	42405470	BB	BB	BB	BB
RS11852412	42409999	ab	ab	BB	BB

RS1712440	42411029	AA	AA	AA	AA
RS4924623	42411189	ab	ab	AA	AA
RS1712439	42411286	AA	AA	AA	AA
RS1712426	42412606	BB	BB	AA	AA
RS2034521	42415270	ab	ab	AA	AA
RS4924626	42423090	ab	ab	AA	AA
RS2899041	42429490	AA	AA	AA	AA
RS650392	42430535	ab	ab	BB	BB
RS3825786	42431142	AA	AA	AA	AA
RS648130	42431683	AA	AA	AA	AA
RS1712442	42502282	BB	BB	BB	BB
RS16972887	42522558	BB	BB	BB	BB
RS16972896	42524104	AA	AA	BB	BB
RS1679012	42528676	ab	ab	AA	AA
RS17694281	42528739	AA	AA	AA	AA
RS8036187	42533879	AA	AA	AA	AA
RS8024732	42570718	BB	BB	BB	BB
RS16972989	42572231	AA	AA	AA	AA
RS34373997	42583801	BB	BB	BB	BB
RS16973015	42585099	AA	AA	AA	AA
RS12914737	42589317	AA	AA	AA	AA
RS2412697	42605791	AA	AA	AA	AA
RS12903690	42615305	AA	AA	AA	AA
RS1659215	42619508	AA	AA	AA	AA
RS16973119	42636303	BB	BB	BB	BB
RS7181742	42643529	AA	AA	AA	AA
RS7180279	42643538	AA	AA	AA	AA
RS3743006	42645768	BB	BB	BB	BB
RS28364384	42666499	BB	BB	BB	BB
RS35249793	42667015	AA	AA	AA	AA
RS28364405	42679414	AA	AA	AA	AA
RS28364409	42679857	AA	AA	AA	AA
RS28364433	42683630	BB	BB	BB	BB
RS28364441	42684875	BB	BB	BB	BB
RS3115877	42688772	BB	BB	BB	BB
RS28364492	42694568	BB	BB	BB	BB
RS28364500	42696606	BB	BB	BB	BB
RS2412711	42697231	BB	BB	BB	BB
RS28364517	42699128	BB	BB	BB	BB
RS3115883	42701688	BB	BB	BB	BB
RS3115884	42703406	BB	BB	BB	BB
RS28364547	42703899	BB	BB	BB	BB
RS28364550	42705007	AA	AA	AA	AA
RS12594633	42705464	AA	AA	AA	AA
RS34192054	42707820	AA	AA	BB	BB
RS28621687	42726693	BB	BB	BB	BB
RS35896246	42727621	BB	BB	BB	BB
RS4924677	42729508	BB	BB	BB	BB

RS34792942	42742435	AA	AA	AA	AA
RS12101559	42742464	AA	AA	AA	AA
RS12440118	42744094	BB	BB	AA	AA
RS16973265	42752542	AA	AA	BB	BB
RS1866396	42755555	AA	AA	AA	AA
RS28491449	42761379	BB	BB	AA	AA
RS4924678	42761436	AA	AA	BB	BB
RS2617237	42765624	BB	BB	AA	AA
RS17709596	42767981	AA	AA	BB	BB
RS6493048	42787459	BB	BB	BB	BB
RS34707422	42826154	BB	BB	AA	AA
RS34359922	42836056	AA	AA	AA	AA
RS876992	42878456	BB	BB	BB	BB
RS28461422	42883883	BB	BB	BB	BB
RS6493054	42886504	AA	AA	AA	AA
RS1667493	42889170	BB	BB	AA	AA
RS17767270	42898612	AA	AA	BB	BB
RS17767439	42927182	AA	AA	AA	AA
RS12594951	42934631	BB	BB	BB	BB
RS16957063	42984288	AA	AA	AA	AA
RS12592374	42991299	AA	AA	AA	AA
RS17774047	43013226	BB	BB	BB	BB
RS12917189	43023482	AA	AA	AA	AA
RS17712677	43041246	AA	AA	AA	AA
RS7181238	43062820	BB	BB	BB	BB
RS11854550	43069014	BB	BB	BB	BB
RS9920562	43073597	AA	AA	AA	AA
RS9920935	43075202	BB	BB	BB	BB
RS10467975	43097652	BB	BB	BB	BB
RS7182753	43109385	BB	BB	AA	AA
RS16957205	43118125	BB	BB	BB	BB
RS17775525	43121684	AA	AA	AA	AA
RS11070382	43151911	AA	AA	AA	AA
RS28810091	43156253	BB	BB	AA	AA
RS16957250	43170823	BB	BB	BB	BB
RS2306126	43235317	AA	--	AA	AA
RS17776090	43235584	AA	AA	AA	AA
RS16957277	43237572	AA	AA	BB	BB
RS35069201	43317071	AA	AA	AA	AA
RS4923956	43338652	BB	BB	AA	AA
RS34018858	43342019	AA	AA	AA	AA
RS4924704	43352041	AA	AA	AA	AA
RS17720890	43385400	BB	BB	AA	AA
RS17721275	43414673	BB	BB	BB	BB
RS7165656	43423203	BB	BB	AA	AA
RS2176870	43436410	AA	AA	BB	BB
RS28365865	43477780	BB	BB	BB	BB
RS530118	43478511	AA	AA	BB	BB

RS17778356	43487810	BB	BB	BB	BB
RS45594236	43494017	BB	BB	BB	BB
RS35985214	43527819	AA	AA	AA	AA
RS34448188	43533193	BB	BB	BB	BB
RS7162827	43538511	BB	BB	BB	BB
RS542036	43541139	AA	AA	BB	BB
RS501884	43553982	BB	BB	AA	AA
RS471122	43558574	AA	AA	BB	BB
RS488756	43614724	AA	AA	BB	BB
RS7048	43620073	AA	AA	AA	AA
RS3917221	43658935	BB	BB	BB	BB
RS2412778	43660982	AA	AA	BB	BB
RS2412781	43667900	AA	AA	BB	BB
RS999047	43688916	AA	AA	BB	BB
RS3883	43695716	BB	BB	BB	BB
RS3742973	43697459	BB	BB	BB	BB
RS45608631	43699889	AA	AA	AA	AA
RS1058298	43700930	BB	BB	AA	AA
RS16957709	43702948	AA	AA	AA	AA
RS2242069	43713634	AA	AA	BB	BB
RS3803339	43724532	AA	AA	AA	AA
RS2602141	43724646	AA	AA	BB	BB
RS16957730	43730486	AA	AA	AA	AA
RS45482998	43733730	AA	AA	AA	AA
RS45470395	43733766	AA	AA	AA	AA
RS689647	43762196	BB	BB	AA	AA
RS17782608	43768642	AA	AA	BB	BB
RS12898231	43782785	AA	AA	AA	AA
RS17782975	43798039	AA	AA	AA	AA
RS3803335	43817225	BB	BB	BB	BB
RS45569034	43818926	BB	BB	BB	BB
RS11635852	43929764	BB	BB	BB	BB
RS12595401	43931682	BB	BB	BB	BB
RS8042868	43939642	BB	BB	BB	BB
RS7175525	43995380	AA	AA	BB	BB
RS2467402	44024490	BB	BB	BB	BB
RS12901165	44036858	BB	BB	BB	BB
RS3087657	44063859	AA	AA	AA	AA
RS35454865	44067985	AA	AA	AA	AA
RS3844075	44068160	BB	BB	BB	BB
RS12702	44093927	AA	AA	AA	AA
RS34623235	44120340	BB	BB	BB	BB
RS678084	44120559	BB	BB	BB	BB
RS2918947	44123073	BB	BB	BB	BB
RS11854565	44148142	BB	BB	BB	BB
RS3742984	44163528	AA	AA	AA	AA
RS12442297	44168470	BB	BB	BB	BB
RS12906333	44170045	AA	AA	AA	AA

RS524908	44187991	AA	AA	AA	AA
RS1439116	44209446	BB	BB	BB	BB
RS1545182	44216110	AA	AA	AA	AA
RS7178452	44242039	BB	BB	BB	BB
RS28431326	44259856	BB	BB	BB	BB
RS17582478	44271206	AA	AA	AA	AA
RS7168522	44314337	BB	BB	BB	BB
RS17504748	44326570	AA	AA	AA	AA
RS4923971	44328112	BB	BB	BB	BB
RS12907002	44347500	AA	AA	AA	AA
RS958485	44350065	BB	BB	BB	BB
RS10459588	44365946	AA	AA	AA	AA
RS12903579	44373887	AA	AA	AA	AA
RS17583428	44380224	BB	BB	AA	AA
RS16959468	44382398	AA	AA	AA	AA
RS2623016	44401266	AA	AA	AA	AA
RS34680070	44433196	BB	BB	BB	BB
RS12910886	44457653	AA	AA	AA	AA
RS17506480	44473172	AA	AA	AA	AA
RS28421746	44481107	BB	BB	BB	BB
RS2706464	44486511	BB	BB	BB	BB
RS7178082	44493567	AA	AA	AA	AA
RS2615260	44505872	BB	BB	BB	BB
RS10400813	44535366	AA	AA	AA	AA
RS8024461	44582886	AA	AA	AA	AA
RS2412864	44598642	AA	AA	AA	AA
RS12595484	44602551	AA	AA	AA	AA
RS1021800	44609796	AA	AA	AA	AA
RS7164866	44635729	AA	AA	AA	AA
RS2055061	44722739	BB	BB	BB	BB
RS10518985	44724287	BB	BB	BB	BB
RS17586255	44728169	AA	AA	AA	AA
RS34732486	44762423	AA	AA	AA	AA
RS2453274	44774202	BB	BB	BB	BB
RS34327950	44778639	BB	BB	BB	BB
RS883943	44788705	BB	BB	BB	BB
RS4611428	44815160	BB	BB	BB	BB
RS2556560	44821843	AA	AA	AA	AA
RS10518980	44822774	AA	AA	AA	AA
RS28409610	44827024	BB	BB	BB	BB
RS17586936	44847394	AA	AA	AA	AA
RS2303578	44849698	BB	BB	BB	BB
RS17586985	44851244	BB	BB	BB	BB
RS12594905	44881964	AA	AA	AA	AA
RS17515394	44898870	AA	AA	AA	--
RS36014111	44900675	BB	BB	BB	BB
RS12594578	44934061	BB	BB	BB	BB
RS3759871	44943757	AA	AA	AA	AA

RS3759875	44943958	AA	AA	AA	AA
RS7165146	44951174	AA	AA	AA	AA
RS12594463	44984631	AA	AA	AA	AA
RS4099	44988610	AA	AA	AA	AA
RS1901530	45005146	BB	BB	BB	BB
RS11553037	45007770	BB	BB	BB	BB
RS2290330	45021227	BB	BB	AA	AA
RS17588305	45021766	AA	AA	BB	BB
RS3759878	45028587	AA	AA	AA	AA
RS2444004	45040512	BB	BB	BB	BB
RS2444006	45043972	BB	BB	BB	BB
RS7182597	45045260	AA	AA	AA	AA
RS2470911	45047134	BB	BB	AA	AA
RS17588988	45047402	AA	AA	AA	AA
RS3759883	45048841	BB	BB	AA	AA
RS7182022	45069742	AA	AA	BB	BB
RS8023560	45072082	BB	BB	AA	AA
RS2462043	45074519	BB	BB	BB	BB
RS1720726	45076085	AA	AA	AA	AA
RS35922426	45078790	BB	BB	BB	BB
RS2049333	45085225	AA	AA	BB	BB
RS1295359	45089019	AA	AA	BB	BB
RS1288092	45090821	AA	AA	AA	AA
RS11856785	45094155	BB	BB	BB	BB
RS2443978	45094624	BB	BB	BB	BB
RS7172822	45094869	BB	BB	BB	BB
RS10152725	45095196	BB	BB	BB	BB
RS17518970	45095902	AA	AA	BB	BB
RS2924123	45096023	BB	BB	AA	AA
RS16974812	45096283	BB	BB	BB	BB
RS16952664	45096539	AA	AA	AA	AA
RS16952671	45097181	AA	AA	BB	BB
RS17592201	45135017	AA	AA	BB	BB
RS956093	45202972	BB	BB	BB	BB
RS13379531	45225352	BB	BB	BB	BB
RS12902975	45267670	AA	AA	AA	AA
RS11635836	45299916	BB	BB	BB	BB
RS199335	45306556	AA	AA	AA	AA
RS7183046	45379702	AA	AA	AA	AA
RS10851420	45385916	BB	BB	BB	BB



Table S1: list of haplotypes from two families with in the shared ROH (chr15:42,254,070-45,702,800).

**Table S2**

<b>Family</b>	<b>Affected (<i>n</i>)</b>	<b>Mutation</b>	<b>ExAC Frequency</b>	<b><i>In silico</i> analysis of pathogenicity</b>
1	2	PATL2 NM_001145112.1:c.478C>T:p.(Arg160*)	0.00003362	Truncation of 383 amino acids
2	2	PATL2 NM_001145112.1:c.1108G>A:p.(Gly370Arg)	0	PolyPhen: possibly_damaging (0.915) SIFT: deleterious (0.03) CADD: 33

**Table S2:** Variants identified in *PATL2* in two families.